

# Simplified SVPWM for Three-Level Inverter Extending Operation into Over Modulation Region

R. Linga Swamy

Assistant Professor, University College of Engineering (A), Osmania University, Hyderabad, India

P. Lokender Reddy

Assistant Professor, University College of Engineering (A), Osmania University, Hyderabad, India

M. Sai Kiran

M.E. Student, University College of Engineering (A), Osmania University, Hyderabad, India

## ABSTRACT

A three-level inverter operated in over modulation region, gives higher speed, higher torque and higher power characteristics. In comparison to a two-level inverter, a three-level inverter has a larger number of switches and is more difficult to implement in the over modulation zone. In this paper, a simplified space vector PWM is proposed for over-modulation region of space vector modulated three level inverter fed induction motor drive. In this method timings are calculated for sector A and the timings for remaining sectors are calculated using mapping, hence number of calculations is reduced and implementation is simplified. The proposed method is verified using MATLAB simulation. In this study, the SVPWM is used in three different regions, including overmodulation region 1 and region 2, and the outcomes are compared.

**Keywords**—over modulation; space vector; linear modulation;

Date of Submission: 01-12-2021

Date of Acceptance: 15-12-2021

## I. INTRODUCTION

THREE-LEVEL voltage-fed PWM inverters are recently showing growing popularity for multi-megawatt industrial drive applications. Sharing of large voltage between the series devices and improvement of harmonic quality at the output compared to a two-level inverter. The rapid development of the capacity and the switching frequency of power semiconductor devices and the continuous advance of the power electronics technology have made many changes in static power converter systems and industrial motor drive areas. Especially, the voltage source PWM inverters have been extending their application area widely due to the increase of gate turn-off (GTO) thyristors capacity and continuing development of industrial provision.

Three-level inverter topology being widely used in high voltage/ high power applications due to its high voltage handling and good harmonic rejection capabilities with currently available power devices like GTOS. Fig.1 shows the basic circuit diagram of three-level inverter excluding detailed snubber circuits and anti parallel diodes. It is known that the three-level inverter roughly has four times

better in harmonics content compared with conventional two-level topology having same number of devices and ratings. So far various PWM techniques controlling three-level inverter have been studied and a good plenty of results are published such as modified two-level triangular carrier modulation, cost function minimizing PWM and space vector. Space vector PWM of a three-level inverter is considerably more complex than that of a two-level inverter because of large number of inverter switching states. In addition, there is the problem of neutral point voltage balancing. Unfortunately, operation in the under modulation range of SVM restricts the drive operation in constant torque region only with voltage modulation factor up to 90.7%. An over modulation strategy of SVM with modulation factor extending from 90.7% to near unity is essential if the drive is required to operate at extended speed including the field-weakening region in vector control with higher torque and power characteristics.

## II. SIMPLIFIED SVPWM IN UNDERMODULATION REGION

A. *Three-Level Topology and switching states*

A three-level GTO inverter is shown schematically in Fig1 . Two clamping diodes, four GTOs, and four

freewheeling diodes make up each phase of the inverter. When the switches  $S_{1A}$  and  $S_{2A}$  are closed, the phase V is in state P (positive bus voltage), and when  $S_{3A}$  and  $S_{4A}$  are closed, it is in state N (negative bus voltage). When the phase is clamped at the neutral point, the phase is in condition O, and either  $S_{2A}$  or  $S_{3A}$  conducts depending on the positive or negative phase current polarity. The three level inverter has  $27(3^3)$  switching states since each phase has three types of switching states and terminal voltages. The space voltage vectors for output voltage are presented in Fig.2. We divide the min into four categories based on the size of the voltage vectors: zero voltage vector ( $V_0$ ), small voltage vectors ( $V_1, V_4, V_7, V_{10}, V_{13}, V_{16}$ ), moderate voltage vectors ( $V_1, V_4, V_7, V_{10}, V_{13}, V_{16}$ ) ( $V_3, V_6, V_9, V_{12}, V_{15}, V_{18}$ ), and Large voltage vector ( $V_2, V_5, V_8, V_{11}, V_{14}, V_{17}$ ) where the P, O, N represent terminal voltage respectively, that is  $V_{dc}/2, 0, -V_{dc}/2$ .

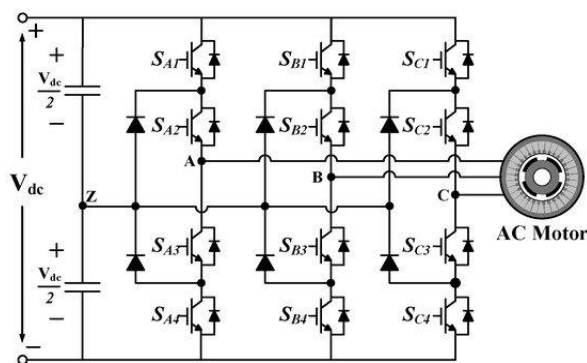


Fig.1. Circuit diagram of 3L NPC inverter

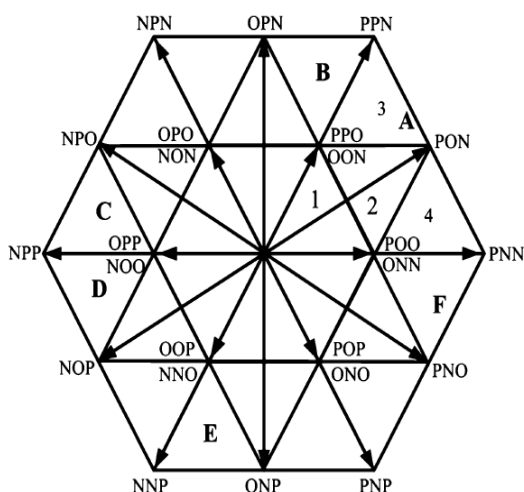


Fig.2. Space vector diagram for Three-Level inverter

**B. Voltage Vector and its Duration**

The triangle produced by the voltage vectors  $V_0, V_2$ , and  $V_5$  is shown in Fig.3. There are four little triangles in this triangle: 1, 2, 3, and 4. In order to minimise the harmonic components of the output voltage and current, the output voltage vector in

space voltage vector PWM is often produced by its nearest three vectors. Vector calculation can be used to determine the duration of each vector. The duration of each voltage vector can be estimated using the following equations if the reference voltage vector falls into the triangle 2.

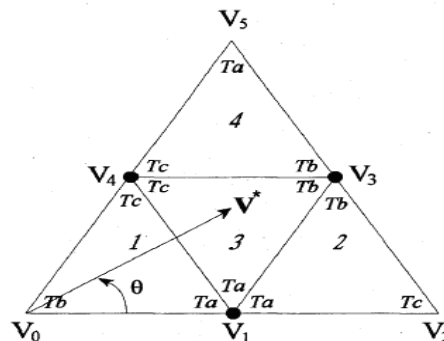


Fig.3.voltage vector in sector 1

$$V_1 T_a + V_3 T_b + V_4 T_c = V^* T_s \quad (1)$$

$$T_a + T_b + T_c = T_s \quad (2)$$

The on of the voltage vectors can be estimated using the formulae above :

$$T_a = T_s [1 - 2k \sin(\theta)] \quad (4)$$

$$T_b = T_s [2k \sin(\theta + 60) - 1] \quad (5)$$

$$T_c = T_s [2k \sin(\theta - 60) + 1] \quad (6)$$

Where  $k = 2V/\sqrt{3}$  The dwelling time in other regions of sector A can be calculated using the same technique, as shown in Table I.

Table I dwelling times for all regions in sector A

Region	$T_a$	$T_b$	$T_c$
1	$2kT_s \sin(60-\theta)$	$T_s [1 - 2k \sin(\theta + 60)]$	$2kT_s \sin(60-\theta)$
2	$2T_s [1 - k \sin(\theta + 60)]$	$2kT_s \sin \theta$	$T_s [2k \sin(60-\theta) - 1]$
3	$T_s [1 - 2k \sin \theta]$	$T_s [2k \sin(\theta + 60) - 1]$	$T_s [2k \sin(\theta - 60) + 1]$
4	$T_s [2k \sin \theta - 1]$	$2kT_s \sin(60-\theta)$	$2T_s [1 - k \sin(\theta + 60)]$

**C. Arrangement for Switching Sequences**

After calculating the on times, the switching sequence must be defined. The converter, however, has some redundant switching states, so there are a few possibilities to choose from. Switching sequence can be arranged according to a specific optimal goal, such as lowest switching loss or total harmonic distortion (THD). In order to achieve reduced THD, every relevant switching is addressed in this study. The switching sequence is made up of states. The Sector A switching sequences are organized as follows[1]:

- Region 1: PPO-POO-OOO-OON-ONN and return
- Region 2: PPO-POO-PON-OON-ONN and return
- Region 3: PPO-PPN-PON-OON and return
- Region 4: POO-PON-PNN-ONN and return

**D. Time setting for each switch**

Switching sequence for region 2 is shown in Fig 4 . As shown in Table II, the time settings for each switch in sector A can be obtained.

Table II

Region	1	2	3	4
S1a	$T_a/4+T_c/4$	$T_a/4+T_b/2+T_c/4$	$T_s/2-T_c/4$	$T_s/2-T_a/4$
S2a	$T_s/2$	$T_s/2$	$T_s/2$	$T_s/2$
S1b	$T_c/4$	$T_c/4$	$T_c/4+T_a/2$	0
S2b	$T_s/2-T_a/4$	$T_s/2-T_a/4$	$T_s/2$	$T_a/4+T_b/2$
S1c	0	0	0	0
S2c	$T_s/2-T_a/4-T_c/4$	$T_c/4+T_a/4$	$T_c/4$	$T_a/4$

The procedures for realizing the above results in sector A can be applied to other sectors with similar results. Figure 4 depicts the calculation flow for the three-level SVPWM. Any reference vector that remains in any position has the same flow, although the voltage vectors and switching patterns are different. Each region has its own set of sequences. So there are 24 routines in total. To complete the three-level SVPWM, you'll need (one procedure for each region).

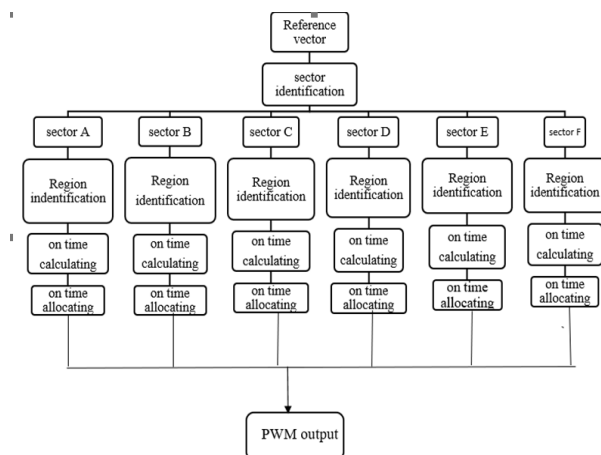


Fig.4 Conventional calculation procedure for three level SVPWM

The fundamental inspiration for the simpler approach comes from the fact that the shapes of the six sectors are identical (see Fig. 2). As a result, there should be some close correlations between on-time computations and switch arrangements in each step. We can calculate the on times for switches in a given sector and then map the on times in that sector to the corresponding on times in other sectors using the relationships between them if the linkages between them can be clearly established.

When the reference vector in other sectors is rotated by  $n\pi/3$  ( $n=1, 2, 3, 4, 5$ ) to sector A, the on times in sector A are equivalent to those in other sectors.

The switching sequences can be arranged in sector A and then mapped to the other sectors if the relationship between the switching sequences in sector A and those in other sectors is drawn by shifting and reversing phase sequences. In other sectors, the relevant reference vector can be created as shown in Table III.

Table III

Sector	Phase voltage A	Phase voltage B	Phase voltage C
A	$U_a$	$U_b$	$U_c$
B	$-U_b$	$-U_c$	$-U_a$
C	$U_c$	$U_a$	$U_b$
D	$-U_a$	$-U_b$	$-U_c$
E	$U_b$	$U_c$	$U_a$
F	$-U_c$	$-U_a$	$-U_b$

Simplified calculation procedure is shown in the Fig .5

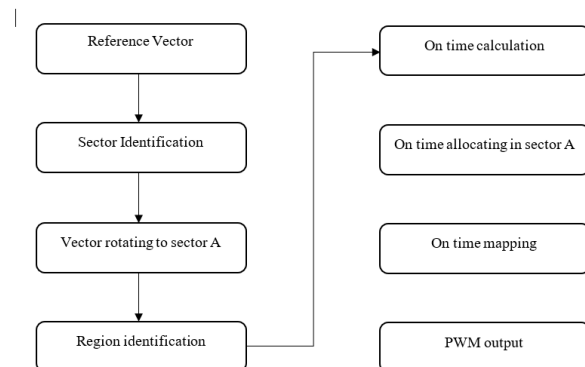


Fig .5. simplified calculation procedure for three level SVPWM

**III. SVM OPERATION EXTENDING INTO OVERMODULATION REGION**

When the reference voltage  $V^*$  surpasses the hexagon border, the inherently nonlinear operation in the overmodulation zone begins. The three-level inverter's SVM overmodulation approach is identical to that of a two-level inverter. Because the theory of overmodulation is the same in all sectors, we will just discuss the procedure for sector A.  $V^*$  crosses the hexagon side at two spots in overmodulation mode-1, as illustrated in Fig.6 for sector A. To compensate for

the loss of fundamental voltage, i.e., to match the output fundamental voltage to the reference voltage, a modified reference voltage trajectory is used that is partly hexagonal and partially circular. The circular component of the trajectory, represented by the segments ab and de, has a larger radius  $V_m^*$  ( $V_m^* > V^*$ ) and intersects the hexagon at an angle, as indicated in the diagram.  $V_m^*$  can be expressed as a function of crossover angle [3] as follows:

$$V_m^* = \frac{2V_d(\frac{\pi}{6} - \theta)}{\pi \sin(\frac{\pi}{6} - \theta)}$$

where  $V_d$  is the voltage across the dc link. The under modulation method, as previously discussed, is still viable in the circular segment. In the ab segment, for example, the inverter vectors  $V_1, V_2$ , and  $V_3$  are chosen for the associated time segments  $T_a, T_b$ , and  $T_c$ . Similarly, for the de segment, the vectors  $V_4, V_3$ , and  $V_5$  are chosen, with  $T_c, T_b$ , and  $T_a$  being the time segments. On the hexagon, the trajectory segment bd can be separated into two parts: bc and cd. Only the vectors  $V_2$ , and  $V_3$  are selected for the corresponding time segments  $T_c$  and  $T_b$  in the bc segment, whereas the vectors  $V_3$  and  $V_5$  are picked for time segments  $T_b$  and  $T_a$  in the cd segment.

When  $V^*$  or  $m$  rises any higher, the overmodulation mode-2 kicks in. Partly keeping the hexagon corner vector for holding angle  $h$  and partly tracking the hexagon side (segments bc and cd) in every sector characterizes the operation in this region, as seen in Fig. 7. During holding angle, the machine phase voltages remain constant, however during hexagon tracking, the voltages fluctuate in a manner similar to mode-1. From Fig. 7, the formula for modified angle  $\alpha$  and  $(\alpha_m)$  can be written as

$$\alpha_m^* = 0 \quad \text{for } 0 < \alpha^* < \alpha_h$$

$$\alpha_m^* = \frac{\alpha^* - \alpha_h}{\frac{\pi}{6} - \alpha_h} \quad \text{for } 0 < \alpha^* < \frac{\pi}{3} - \alpha_h$$

$$\alpha_m^* = \frac{\pi}{3} \quad \text{for } \frac{\pi}{3} - \alpha_h < \alpha^* < \frac{\pi}{3}$$

In order to maintain a three-level output voltage wave, the greatest modulation factor ( $m$ ) of a three-level inverter should be kept to slightly less than one ( $1-\epsilon$ ).

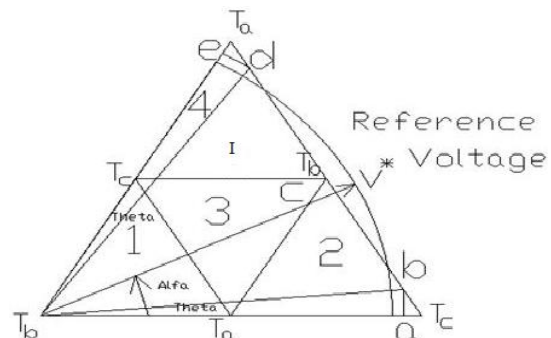


Fig.6. overmodulation mode I

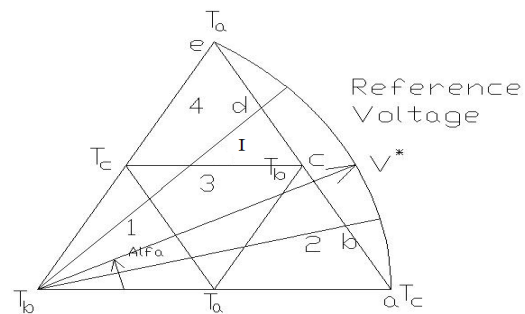


Fig.7. overmodulation mode II

A. Time calculations for space vectors

As previously stated, a major portion of operation occurs on the hexagon side in the sections bc in region 2 and cd in region 4 during mode 1 of the overmodulation area. These sections' analytical formulations for time segments will now be generated. Consider the case where the reference voltage  $V^*$  follows the section bc in area 2 as shown in Fig. 6. The general trajectory angle  $\theta_e$  has taken the place of the sector angle. For space vector PWM, the following two equations should be valid:

$$V_2 * T_b + V_3 * T_c = V^* * \frac{T_s}{2} \quad (3)$$

$$T_c + T_b = \frac{T_s}{2} \quad (4)$$

$T_s$  is the sampling time. As illustrated in the diagram, the voltage  $V^*$  can be broken down into two component vectors:  $V_A$  and  $V_B$ . We can write Sector A, Region 2: based on the geometry.

$$\frac{V_b}{\sin \theta} = \frac{V^*}{\sin 150} = 2 * V^* \quad (5)$$

$$\frac{V_2}{\sin(120 - \theta_e)} = \frac{V^*}{\sin 60} = \frac{2}{\sqrt{3}} * V^* \quad (6)$$

$$V_A = V^* * \cos \theta_e - V_B \cos 30 \quad (7)$$

Substituting (1) and (2) in (3) and simplifying, we get

$$V_A = V_2 \frac{\sqrt{3} \cos \theta_e - 3 \sin \theta_e}{\sqrt{3} \cos \theta_e + 3 \sin \theta_e} \quad (8)$$

since

$$\frac{T_c}{0.5T_s} = \frac{V_A}{V_2}$$

We can write

$$T_c = \frac{T_s}{2} * \frac{\sqrt{3} \cos \theta_e - 3 \sin \theta_e}{\sqrt{3} \cos \theta_e + 3 \sin \theta_e} \quad (9)$$

Therefore, to establish, the vector has to be impressed for the time segment

$$T_b = \frac{T_s}{2} - T_c \quad (10)$$

as given by (4). Similar derivations were made for region 2 and 4 in all the six sectors. The resulting expressions are summarized in the second column of Table IV[2].

Table IV: Dwell Times for in region 2 and 4 of over modulation region

Sect or	Time segments(region2)	Time segments (region4)
---------	------------------------	-------------------------

REGION	STATES	SWITCHING STATES
1.2	17-16	PON-PNN
1.4	18-17	PPN-PON
1	$T_c = \frac{T_s}{2} \left( \frac{\sqrt{3} \cos \theta_e - 3 \sin \theta_e}{\sqrt{3} \cos \theta_e + \sin \theta_e} \right)$ $T_b = \frac{T_s}{2} - T_c$	$T_b = \frac{T_s}{2} \left( \frac{2\sqrt{3} \cos \theta_e - 2 \sin \theta_e}{\sqrt{3} \cos \theta_e + \sin \theta_e} \right)$ $T_a = \frac{T_s}{2} - T_b$
2	$T_a = \frac{T_s}{2} \left( \frac{\sqrt{3} \cos \theta_e}{\sin \theta_e} \right)$ $T_b = \frac{T_s}{2} - T_a$	$T_b = \frac{T_s}{2} \left( \frac{\sin \theta_e + \sqrt{3} \sin \theta_e}{\sin \theta_e} \right)$ $T_c = \frac{T_s}{2} - T_b$
3	$T_c = \frac{T_s}{2} \left( \frac{\sqrt{3} \cos \theta_e + 3 \sin \theta_e}{\sin \theta_e - \sqrt{3} \cos \theta_e} \right)$ $T_b = \frac{T_s}{2} - T_c$	$T_b = \frac{T_s}{2} \left( \frac{4 \sin \theta_e}{\sin \theta_e - \sqrt{3} \cos \theta_e} \right)$ $T_a = \frac{T_s}{2} - T_b$
4	$T_a = \frac{T_s}{2} \left( \frac{\sqrt{3} \cos \theta_e + 3 \sin \theta_e}{\sqrt{3} \cos \theta_e + \sin \theta_e} \right)$ $T_b = \frac{T_s}{2} - T_a$	$T_b = \frac{T_s}{2} \left( \frac{2\sqrt{3} \cos \theta_e - 2 \sin \theta_e}{\sqrt{3} \cos \theta_e + \sin \theta_e} \right)$ $T_a = \frac{T_s}{2} - T_b$
5	$T_c = \frac{T_s}{2} \left( \frac{\sqrt{3} \cos \theta_e}{\sin \theta_e} \right)$ $T_b = \frac{T_s}{2} - T_c$	$T_b = \frac{T_s}{2} \left( \frac{\sin \theta_e + \sqrt{3} \sin \theta_e}{\sin \theta_e} \right)$ $T_a = \frac{T_s}{2} - T_b$
6	$T_a = \frac{T_s}{2} \left( \frac{\sqrt{3} \cos \theta_e + 3 \sin \theta_e}{\sin \theta_e - \sqrt{3} \cos \theta_e} \right)$ $T_b = \frac{T_s}{2} - T_a$	$T_b = \frac{T_s}{2} \left( \frac{4 \sin \theta_e}{\sin \theta_e - \sqrt{3} \cos \theta_e} \right)$ $T_c = \frac{T_s}{2} - T_b$

#### IV. PROPOSED SIMPLIFIED SVM FOR OVERMODULATION REGION

Simplified SVPWM is given in section II for under modulation region. In the proposed method, it is applied to over modulation region. Fig. 8 shows the timing diagram for over modulation, mode II. Switching pattern for region 2 and 4 of sector A is given in Table V. From Fig. 8 switching times for each switch of region 2 and 4 are calculated and is given in Table VI

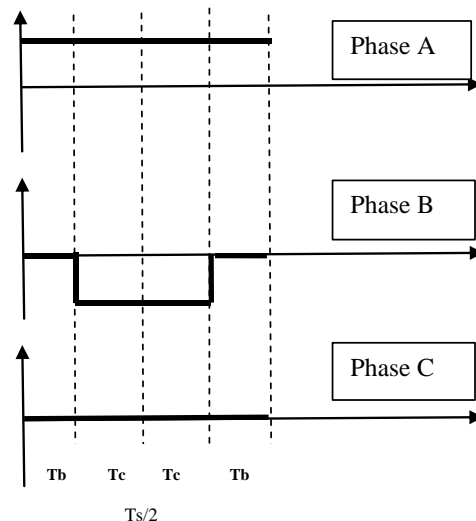


Fig.8. Timing diagram for over modulation mode II

Table V  
SWITCHING PATTERN FOR SECTOR A

Table VI  
TURN ON TIMES OF ALL SWITCHES FOR REGION 5 AND 6

Region	2	4
SA1	Ts/2	Ts/2
SA2	Ts/2	Ts/2
SB1	0	Ta
SB2	Tb	Ts/2
SC1	0	0
SC2	0	0

Once turn on time is calculated for sector A, turn on times for remaining sectors are calculated using mapping method given in section II.

In a similar way turn times are also calculated for over modulation region mode I. These turn times are compared with carrier wave to generate switching pulses for three level inverter.

C . Implementation of simplified SVPWM for 3-level NPC inverter fed induction motor

Induction machine model taken from MATLAB and simplified SVPWM is tested with simulation. The machine parameters details are given in table VII. Fig.9 shows the Simulink model for simplified space vector PWM for 3-PWM for 3-level inverter fed induction motor in both overmodulation and under modulation regions. In this model the complete operation of space vector PWM in both regions takes place. Fig.10 shows the Simulink model of the gating signal developed for 3-level inverter. MATLAB program to generate switching signal for Space vector PWM of 3-level inverter fed induction motor for over modulation region Mode I and II is developed using code written in MATLAB function block then parameters like line voltages, phase voltages ,torque , speed are compared in all modes of operation.

Table VII: SPECIFIATIONS OF INDUCTION MOTOR

parameter	Value
Rated voltage	200v
Rated frequency	50HZ
Rated power	1545W
poles	4

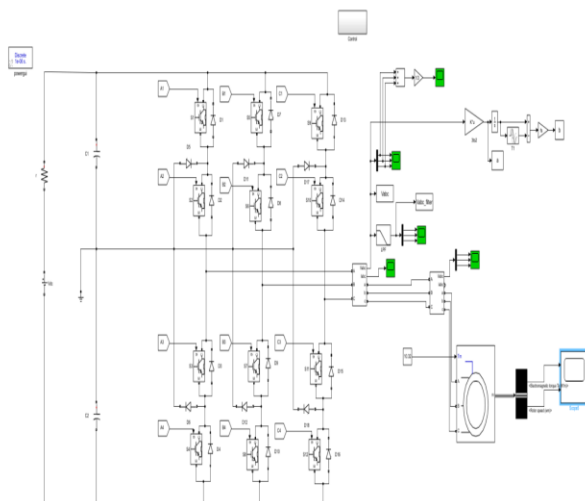


Fig.9. Three-level inverter connected to load

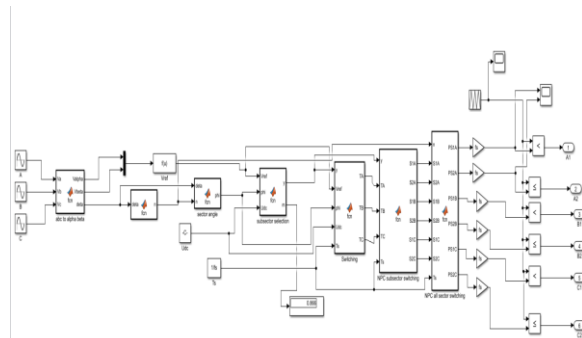


fig.10. control circuit

V. SIMULATION RESULTS

In this section simulation results are given in under modulation and over modulation regions (Mode I and II).

Fig 11, 14 and 17 shows the Electrical torque and speed at load torque at 10.32N-m in under modulation and over modulation regions (Mode I and II) respectively. Fig 12 , 15 and 18 shows Machine line voltages  $V_{ab}$ ,  $V_{bc}$ ,  $V_{ca}$  in under modulation and over modulation regions (Mode I and II) respectively. Fig 13,16 and 19 shows the Machine Phase currents  $I_a$ ,  $I_b$ ,  $I_c$  . in under modulation and over modulation regions (Mode I and II) respectively.

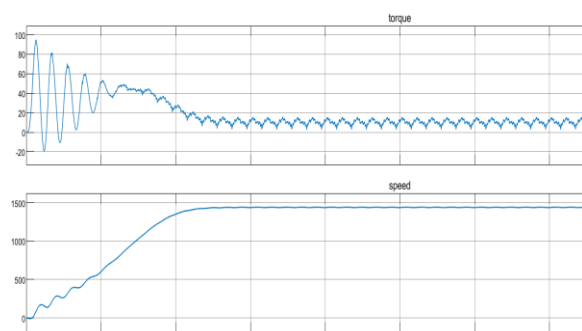


Fig 11 Electrical Torque and Speed. (Vs) Time (vs) time in under modulation region



Fig.12 Machine line voltages of  $V_{ab}$ ,  $V_{bc}$ ,  $V_{ca}$  in under modulation region

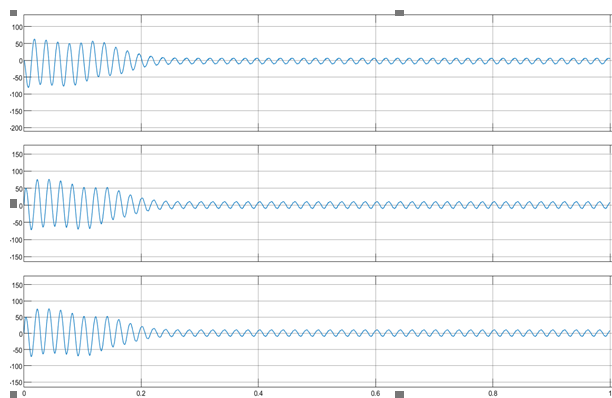


Fig.13 Machine Phase currents  $I_a$ ,  $I_b$ ,  $I_c$  in under modulation region

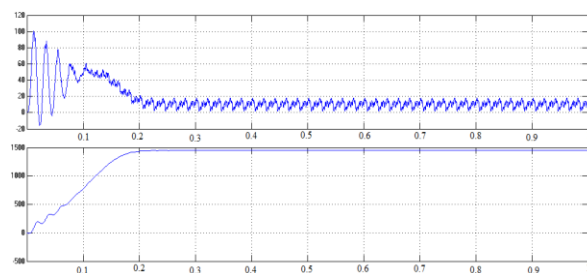


Fig.14 Electrical Torque and Speed.(Vs) Time in overmodulation region I

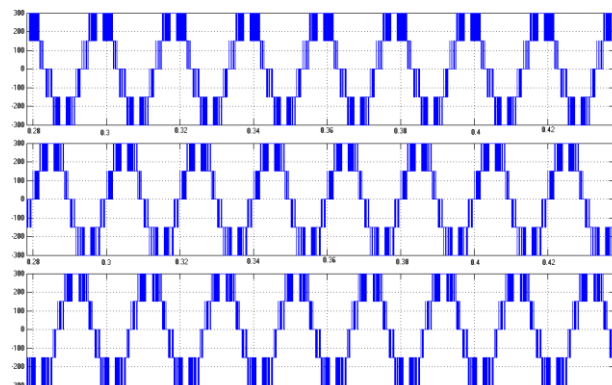


Fig.15 Machine line voltages of  $V_{ab}$ ,  $V_{bc}$ ,  $V_{ca}$  in over modulation region I

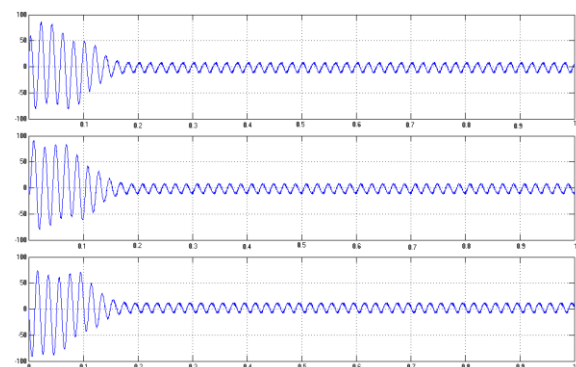


Fig.16 Phase currents  $I_a$ ,  $I_b$ ,  $I_c$  in overmodulation region I

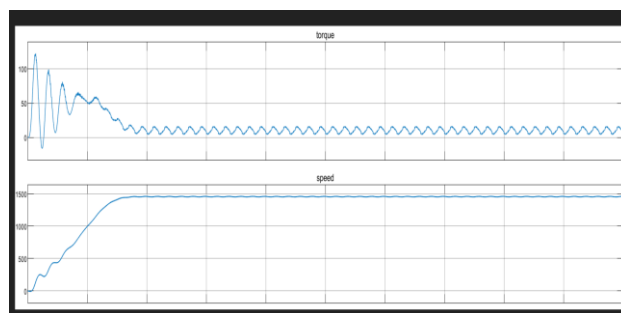


Fig.17 Electrical Torque and Speed(Vs)Time in overmodulation region II

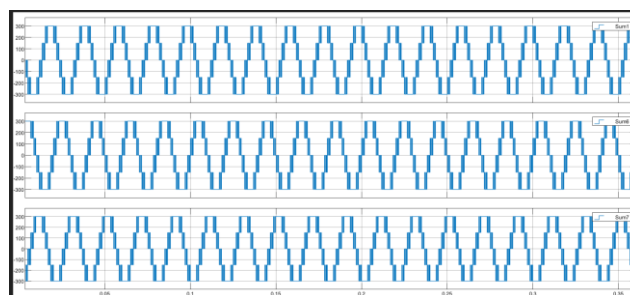


Fig.18 Machine line voltages of  $V_{ab}$ ,  $V_{bc}$ ,  $V_{ca}$  in over modulation region II

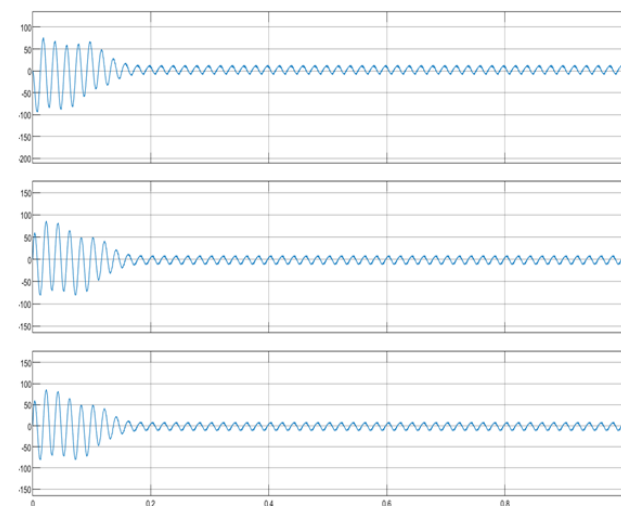


Fig. 19 Phase currents  $I_a$ ,  $I_b$ ,  $I_c$  in overmodulation region II

Table VII shows the performance parameters for under modulation and over modulation regions (Mode I and II). Overmodulation region shows the improvement of improvement in speed, voltage and torque.

Table VII

Region of operation	Under modulation	Over modulation I	Over modulation II
Voltage	300	300	300
speed	1440	1450	1461
$V_{rms}$	201.3	204.9	229.5

$I_{rms}$	6.352A	6.69A	6.808A
THD % of current	13.05	19.01	19.11
Torque	10.32	11.04	11.34

## VI. CONCLUSION

A new simplified Space Vector PWM Algorithm is proposed and Verified by Simulation of a space vector PWM of three level inverter fed induction motor drive operation in Over modulation region and under modulation region. Speed,  $V_{rms}$ ,  $I_{rms}$  is gradually increased from under modulation to over modulation region II. So, it is useful in applications particularly where large speeds are required instantly.

$V_{rms}$  increases by nearly 15% from under modulation region to over modulation region II, where as 2% in over modulation region I. Speed increases by 21RPM from under modulation region to over modulation region II, Where as 10RPM in under modulation region.  $I_{rms}$  increases by 0.5A from under modulation region to over modulation region II, where as 0.3A in over modulation region I

## REFERENCES

- [1]. Hu, H., Yao, W., & Lu, Z. (2007). Design and implementation of three-level space vector PWM IP core for FPGAs. *IEEE Transactions on power electronics*, 22(6), 2234-2244.
- [2]. Subrata K. Mondal, Bimal K. Bose, Valentin Oleschuk, and Joao O. P. Pinto, "Space vector pulse width modulation of three level inverter extending operation into overmodulation region", *IEEE Transaction on Power Electronics*, Vol. 18, No. 2, March 2003
- [3]. M. Koyama, T. Fujii, R. Uchida, and T. Kawabata, "Space voltage vector based new PWM method for large capacity three-level GTO inverter," in *Proc. IEEE IECON Conf.*, 1992, pp. 271-276.
- [4]. Y. H. Lee, B. S. Suh, and D. S. Hyun, "A novel PWM scheme for a three-level voltage source inverter with GTO thyristors," *IEEE Trans. Ind. Applicat.*, vol. 32, pp. 260-268, Mar./Apr. 1996.
- [5]. S. K. Mondal, J. O. P. Pinto, and B. K. Bose, "A neural-network-based space vector PWM controller for a three-level voltage-fed inverter induction motor drive," *IEEE Trans. Ind. Applicat.*, vol. 38, pp. 660-669, May/June 2002.
- [6]. J. O. P. Pinto, B. K. Bose, L. E. B. da Silva, and M. P. Kazmierkowski, "A neural network based space vector PWM controller for voltage-fed inverter induction motor drive," *IEEE Trans. Ind. Applicat.*, vol. 36, pp.1628-36, Nov./Dec. 2000.
- [7]. B. Belkacem, et al., "A Comparative Study Between the Nearest Three Vectors and Two-Level Hexagons Based Space Vector Modulation Algorithms for Three-Level NPC Inverters," *Journal of Power Technologies*, vol. 97, no. 3, pp. 190-200, 2017
- [8]. J. Rodríguez, et al., "Multilevel inverters: a survey of topologies, controls and applications," *IEEE Trans. Ind. Electron.*, vol. 49, no. 4, pp. 724-738, Aug 2002.
- [9]. C. Hu, et al., "An Improved Virtual Space Vector Modulation Scheme for Three-Level Active Neutral-Point-Clamped Inverter," *IEEE Transactions on Power Electronics*, vol. 32, no. 10, pp. 7419-7434, Oct 2017.